A Comparison of Hydrodynamic Damping Models using Least-Squares and Adaptive Identifier Methods for Autonomous Underwater Vehicles

Scott B. Gibson[1], Brian McCarter[2], Daniel J. Stilwell[1] and Wayne L. Neu[3]
Bradley Department of Electrical and Computer Engineering, Virginia Tech[1]
Department of Aerospace and Ocean Engineering, Virginia Tech[3]
Naval Oceanographic Office, Stennis Space Center, Mississippi[2]
{sgibson2, stilwell, neu}@vt.edu
brian.mccarter.ctr@navy.mil

***Abstract*—This work provides a comparison of eight different hydrodynamic damping models for streamlined tail-controlled autonomous underwater vehicles (AUVs). We use an off-line least-squares method and an adaptive identifier method to approximate damping model coefficients and determine if one damping model is preferred over other models. We evaluate the two methods for estimating the parameters of the models. Our initial results show that both identification methods produce similar results, and thus the adaptive identifier might be preferred for some applications because it does not require angular acceleration. Our results also show that the linear damping model has comparable performance to more complex models but employs fewer parameters. We conclude that the linear damping model is preferred over other models due to its simplicity.**

I. Introduction

This work provides a comparison of various hydrodynamic damping models for autonomous underwater vehicles (AUVs). Damping models represent the forces and moments on an AUV due to hydrodynamic damping and can be included in an overall six degree of freedom (6DOF) dynamic model. We seek to determine if one damping model is preferred over other models for the case of streamlined AUVs, and we further evaluate two different methods for estimating the parameters of the models.

We use an off-line least-squares method and an adaptive identifier method to approximate damping model coefficients. Measurement of angular acceleration is required for the least-squares method. If angular acceleration is not directly measured, then it must be inferred from other measurements. The adaptive identifier method we use is a specialization of the adaptive identifier proposed in [1]. The adaptive identifier has some advantages over the least-squares method; it can be implemented on the AUV as an online estimator, and it does not require the measurements of the vehicle's angular acceleration. We present a local stability proof for the adaptive identifier based on the corresponding proof in [1]. The proof guarantees that the linear and angular velocity estimates asymptotically converge to the measured velocities and guarantees that the approximated damping parameter coefficients are bounded.

We compare eight different viscous hydrodynamic damping models found in the literature that we label: McFarland-Whitcomb [1], pitch-yaw, Gertler-Hagen [2], linear, Coe [3], Prestero [4], uncoupled, and Fossen [5]. The McFarland-Whitcomb damping model is fully coupled and assumes a sign-preserved quadratic relationship between velocity and force. The pitch-yaw model is constructed by superimposing separate models for pitch and yaw. The Gertler-Hagen model is a lumped-parameter model which makes no distinction between different physical contributions in the model structure. The linear model assumes a linear relationship between velocity and force. The Coe model is based on a Taylor series expansion and assumes port/starboard vehicle symmetry. The Prestero model includes axial drag, crossflow drag, and body lift. The uncoupled model assumes that motion in each axis is only dependent on velocity along that axis. The Fossen model is uncoupled, but retains both linear and quadratic terms. We include a way to represent different models with the same equations of motion.

Our results show that both identification methods produce similar results, and thus the adaptive identifier might be preferred for some applications because it does not require angular acceleration. Our results also show that the linear damping model has comparable performance to more complex models but employs fewer parameters. We conclude that the linear damping model is preferred over other models due to its simplicity.

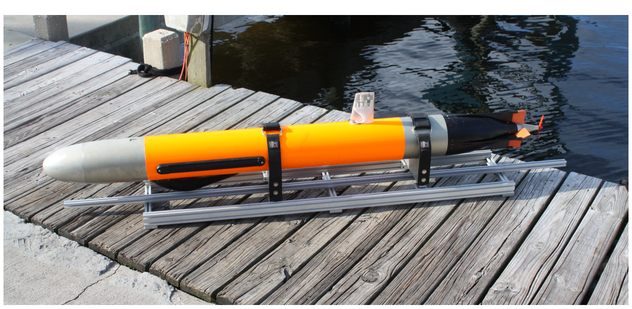

Fig. 1. Virginia Tech 690 AUV

978-0-933957-43-5 ©2015 MTS

II. Problem Statement

A. Equations of Motion

We formulate the rigid body AUV equations of motion as in [1] and [5]. Let $\eta_1 = [x\ y\ z]^\mathsf{T}$ represent the AUV's inertial position, and let $\eta_2 = [\phi\ \theta\ \psi]^\mathsf{T}$ be the attitude of the AUV represented using euler angles. Let $\nu = [u\ v\ w]^\mathsf{T}$ represent the AUV body frame linear velocity, and let $\omega = [p\ q\ r]^\mathsf{T}$ be the body angular velocity. We define $\eta = [\eta_1^\mathsf{T}\ \eta_2^\mathsf{T}]^\mathsf{T}$ and $v = [\nu^\mathsf{T}\ \omega^\mathsf{T}]^\mathsf{T}$ where $\eta,\, v \in \mathbb{R}^{6\times1}$. We model the AUV with added mass, Coriolis, drag, gravitational, buoyancy and control forces. The dynamic model for the AUV in the body frame is

$$M\dot{v} = \mathcal{H}(Mv)v + \tau(v) + \mathcal{G}(R) + u \tag{1}$$

where $\mathcal{G}(R) = \begin{bmatrix} (g+b)R^\mathsf{T}e_3 \\ r_G \times (gR^\mathsf{T}e_3) + r_B \times (bR^\mathsf{T}e_3) \end{bmatrix}$, $e_3 = \begin{bmatrix} 0 \\ 0 \\ 1 \end{bmatrix}$, $R \in SO(3)$ is the rotation from the body frame to the inertial frame, $g \in \mathbb{R}$ is the gravitational force on the vehicle, $b \in \mathbb{R}$ is the buoyancy force on the vehicle, $r_G \in \mathbb{R}^{3\times1}$ is the vehicle's center of gravity position, $r_B \in \mathbb{R}^{3\times1}$ is the vehicle's center of buoyancy position, $M \in \mathbb{R}^{6\times6}$ is the mass matrix, $\tau(v) \in \mathbb{R}^{6\times1}$ represents the damping forces and moments and is discussed in Section II-B, $u \in \mathbb{R}^{6\times1}$ represents the forces and moments experienced from the control surfaces and propeller. The functions $\mathcal{J} : \mathbb{R}^3 \to \mathbb{R}^{3\times3}$ and $\mathcal{H} : \mathbb{R}^6 \to \mathbb{R}^{6\times6}$ are

$$\mathcal{J}\left(\begin{bmatrix} \omega1 \\ \omega2 \\ \omega3 \end{bmatrix}\right) = \begin{bmatrix} 0 & -\omega_3 & \omega_2 \\ \omega_3 & 0 & -\omega_1 \\ -\omega_2 & \omega_1 & 0 \end{bmatrix},$$
$$\mathcal{H}\left(\begin{bmatrix} \nu \\ \omega \end{bmatrix}\right) = \begin{bmatrix} 0_{3\times3} & \mathcal{J}(\nu) \\ \mathcal{J}(\nu) & \mathcal{J}(\omega) \end{bmatrix}.$$

Assumption 1. *The model has the following characteristics:*

(a) The variables η and v are instrumented and measured in real-time.
(b) The variable $\dot{v}$ is instrumented and measured in real-time.
(c) The bounded input u produces bounded output signals η and v.
(d) The mass matrix M, which represents both the inertial mass and the hydrodynamic added mass, is symmetric positive-definite, constant, and known.
(e) The gravitational force g and buoyancy force b are known and constant.
(f) The forces and moments u due to the control surfaces and propeller are known.

B. Damping Model Structure

In order to compare various damping models, we implement the following damping model structure. Let

$$\tau(v) = \begin{bmatrix} \tau^{\mathrm{X}}(v) \\ \tau^{\mathrm{Y}}(v) \\ \tau^{\mathrm{Z}}(v) \\ \tau^{\mathrm{K}}(v) \\ \tau^{\mathrm{M}}(v) \\ \tau^{\mathrm{N}}(v) \end{bmatrix} \tag{2}$$

model damping forces and moments on the AUV. We express each scalar function in (2) as a linear combination of basis functions, which represent all possible combinations of linear and angular velocity for which force and moment due to hydrodynamic damping might be dependent. For example, the heave force $\tau^{\mathrm{Z}}(v)$ might be modeled as a function of heave velocity w and sway velocity v, $\tau^{\mathrm{Z}}(v) = \mathrm{Z_v}v + \mathrm{Z_w}w$, which can be expressed as

$$\tau^{\mathrm{Z}}(v) = K^{\mathrm{Z}}\xi^{\mathrm{Z}}(\nu)$$

with coefficients $K^{\mathrm{Z}} = [0\ \mathrm{Z_v}\ \mathrm{Z_w}]$ and velocity basis functions $\xi^{\mathrm{Z}}(\nu) = [u\ v\ w]^\mathsf{T}$. A generic damping model can be expressed as

$$\begin{aligned}\tau(v) &= \begin{bmatrix} \tau^{\mathrm{X}}(v) \\ \tau^{\mathrm{Y}}(v) \\ \tau^{\mathrm{Z}}(v) \\ \tau^{\mathrm{K}}(v) \\ \tau^{\mathrm{M}}(v) \\ \tau^{\mathrm{N}}(v) \end{bmatrix} = \begin{bmatrix} K^{\mathrm{X}}\xi(v) \\ K^{\mathrm{Y}}\xi(v) \\ K^{\mathrm{Z}}\xi(v) \\ K^{\mathrm{K}}\xi(v) \\ K^{\mathrm{M}}\xi(v) \\ K^{\mathrm{N}}\xi(v) \end{bmatrix} = \begin{bmatrix} K^{\mathrm{X}} \\ K^{\mathrm{Y}} \\ K^{\mathrm{Z}} \\ K^{\mathrm{K}} \\ K^{\mathrm{M}} \\ K^{\mathrm{N}} \end{bmatrix}\xi(v) \\ &= K\xi(v)\end{aligned}$$

where $\xi(v) \in \mathbb{R}^{n_\xi\times1}$ is a vector that includes all n_ξ basis functions from all the damping models and $K \in \mathbb{R}^{6\times n_\xi}$ is the damping coefficient matrix. Each damping model has a unique K that selects the appropriate basis functions from $\xi(v)$.

Assumption 2. *The damping coefficient matrix and vector of basis functions have the following characteristics:*

(a) The damping coefficient matrix, $K \in \mathbb{R}^{6\times n_\xi}$, is constant and unknown.
(b) The vector of basis functions, $\xi(v) \in \mathbb{R}^{n_\xi\times1}$, is bounded if v is bounded.

C. Damping Models

Viscous hydrodynamic damping models describe the dissipative forces caused by drag, body oscillations, and vortex shedding [5]. We present several damping models that vary in complexity.

1) Linear: The linear damping model assumes a linear relationship between velocity and damping forces and moments,

$$\tau^{\mathrm{X}}(v) = \mathrm{X_u}u + \mathrm{X_v}v + \mathrm{X_w}w + \mathrm{X_p}p + \mathrm{X_q}q + \mathrm{X_r}r$$

where damping forces and moments τ^{Y}, τ^{Z}, τ^{K}, τ^{M}, and τ^{N} are defined by replacing X with Y, Z, K, M, and N.

2) McFarland-Whitcomb: The McFarland-Whitcomb damping model [1] is fully coupled and assumes a sign-preserved quadratic relationship between velocity and force.

$$\tau(v) = K_{\mathrm{v|v|}}\mathrm{diag}(v)|v|$$

where $K_{\mathrm{v|v|}}$ is the coupled quadratic drag matrix.

3) Pitch-yaw: The pitch-yaw damping model is constructed by superimposing separate models for pitch and yaw. Note that the model assumes no x-axis damping moment will occur due to velocity which means $\tau^{\mathrm{K}}(v)$ has no coefficients.

$$\begin{aligned}\tau^{\mathrm{X}}(v) = {} & \mathrm{X_q} q + \mathrm{X_r} r + \mathrm{X_u} u + \mathrm{X_v} v + \mathrm{X_w} w + \mathrm{X_{qq}} q^2 \\ & + \mathrm{X_{|r|}} |r| + \mathrm{X_{uu}} u^2 + \mathrm{X_{vv}} v^2 + \mathrm{X_{ww}} w^2 + \mathrm{X_{|v|}} |v| \\ & + \mathrm{X_{u|r|}} u|r| + \mathrm{X_{q|w|}} q|w| + \mathrm{X_{r|v|}} r|v| + \mathrm{X_{v|r|}} v|r| \\ & + \mathrm{X_{w|q|}} w|q| + \mathrm{X_{u|v|}} u|v| + \mathrm{X_{u|w|}} u|w| + \mathrm{X_{v|v|}} v|v| \\ & + \mathrm{X_{w|w|}} w|w| + \mathrm{X_{ur}} ur + \mathrm{X_{vr}} vr + \mathrm{X_{wq}} wq + \mathrm{X_{uv}} uv \\ & + \mathrm{X_{uw}} uw + \mathrm{X_{q|q|}} q|q| + \mathrm{X_{r|r|}} r|r| + \mathrm{X_{q|u|}} q|u| \\ & + \mathrm{X_{u|q|}} u|q|\end{aligned}$$

$$\begin{aligned}\tau^{\mathrm{Y}}(v) = {} & \mathrm{Y_r} r + \mathrm{Y_v} v + \mathrm{Y_{rr}} r^2 + \mathrm{Y_{|r|}} |r| + \mathrm{Y_{uu}} u^2 + \mathrm{Y_{vv}} v^2 \\ & + \mathrm{Y_{|u|}} |u| + \mathrm{Y_{|v|}} |v| + \mathrm{Y_{u|r|}} u|r| + \mathrm{Y_{r|v|}} r|v| \\ & + \mathrm{Y_{v|r|}} v|r| + \mathrm{Y_{u|v|}} u|v| + \mathrm{Y_{v|v|}} v|v| + \mathrm{Y_{ur}} ur \\ & + \mathrm{Y_{vr}} vr + \mathrm{Y_{uv}} uv + \mathrm{Y_{r|r|}} r|r|\end{aligned}$$

where damping moment τ^{N} is defined by replacing Y with N.

$$\begin{aligned}\tau^{\mathrm{Z}}(v) = {} & \mathrm{Z_q} q + \mathrm{Z_w} w + \mathrm{Z_{qq}} q^2 + \mathrm{Z_{|q|}} |q| + \mathrm{Z_{uu}} u^2 + \mathrm{Z_{|u|}} |u| \\ & + \mathrm{Z_{ww}} w^2 + \mathrm{Z_{|w|}} |w| + \mathrm{Z_{u|q|}} u|q| + \mathrm{Z_{q|w|}} q|w| \\ & + \mathrm{Z_{w|q|}} w|q| + \mathrm{Z_{u|w|}} u|w| + \mathrm{Z_{w|w|}} w|w| + \mathrm{Z_{uq}} uq \\ & + \mathrm{Z_{wq}} wq + \mathrm{Z_{uw}} uw + \mathrm{Z_{q|q|}} q|q|\end{aligned}$$

where damping moment τ^{M} is defined by replacing Z with M.

$$\tau^{\mathrm{K}}(v) = 0$$

4) Gertler-Hagen: The Gertler-Hagen damping model, as proposed in [2], is a lumped-parameter model which makes no distinction between different physical contributions in the model structure.

$$\begin{aligned}\tau^{\mathrm{X}}(v) = {} & \mathrm{X_{qq}} q^2 + \mathrm{X_{rr}} r^2 + \mathrm{X_{uu}} u^2 + \mathrm{X_{vv}} v^2 + \mathrm{X_{ww}} w^2 \\ & + \mathrm{X_{vv\overline{\eta}}} v^2(\overline{\eta} - 1) + \mathrm{X_{ww\overline{\eta}}} w^2(\overline{\eta} - 1) + \mathrm{X_{pr}} pr \\ & + \mathrm{X_{vr}} vr + \mathrm{X_{wq}} wq\end{aligned}$$

$$\begin{aligned}\tau^{\mathrm{Y}}(v) = {} & \mathrm{Y_{uu}} u^2 + \mathrm{Y_{vV}} v\mathrm{V} + \mathrm{Y_{pq}} pq + \mathrm{Y_{qr}} qr + + \mathrm{Y_{up}} up \\ & + \mathrm{Y_{ur}} ur + \mathrm{Y_{vq}} vq + \mathrm{Y_{wp}} wp + \mathrm{Y_{wr}} wr + \mathrm{Y_{uv}} uv \\ & + \mathrm{Y_{vw}} vw + \mathrm{Y_{|r|V_v}} |r|\mathrm{V_v} + \mathrm{Y_{p|p|}} p|p| \\ & + \mathrm{Y_{vV\overline{\eta}}} v\mathrm{V}(\overline{\eta} - 1) + \mathrm{Y_{ur\overline{\eta}}} ur(\overline{\eta} - 1) + \mathrm{Y_{uv\overline{\eta}}} uv(\overline{\eta} - 1)\end{aligned}$$

$$\begin{aligned}\tau^{\mathrm{Z}}(v) = {} & \mathrm{Z_{pp}} p^2 + \mathrm{Z_{rr}} r^2 + \mathrm{Z_{uu}} u^2 + \mathrm{Z_{vv}} v^2 + \mathrm{Z_{u|w|}} u|w| \\ & + \mathrm{Z_{wV}} w\mathrm{V} + \mathrm{Z_{pr}} pr + \mathrm{Z_{uq}} uq + \mathrm{Z_{vp}} vp + \mathrm{Z_{vr}} vr \\ & + \mathrm{Z_{uw}} uw + \mathrm{Z_{|q|V_w}} |q|\mathrm{V_w} + \mathrm{Z_{|w|V}} |w|\mathrm{V} \\ & + \mathrm{Z_{wV\overline{\eta}}} w\mathrm{V}(\overline{\eta} - 1) + \mathrm{Z_{uq\overline{\eta}}} uq(\overline{\eta} - 1) \\ & + \mathrm{Z_{uw\overline{\eta}}} uw(\overline{\eta} - 1)\end{aligned}$$

$$\begin{aligned}\tau^{\mathrm{K}}(v) = {} & \mathrm{K_{uu}} u^2 + \mathrm{K_{uu\overline{\eta}}} u^2(\overline{\eta} - 1) + \mathrm{K_{vV}} v\mathrm{V} + \mathrm{K_{pq}} pq \\ & + \mathrm{K_{qr}} qr + \mathrm{K_{up}} up + \mathrm{K_{ur}} ur + \mathrm{K_{vq}} vq + \mathrm{K_{wp}} wp \\ & + \mathrm{K_{wr}} wr + \mathrm{K_{uv}} uv + \mathrm{K_{vw}} vw + \mathrm{K_{p|p|}} p|p|\end{aligned}$$

$$\begin{aligned}\tau^{\mathrm{M}}(v) = {} & \mathrm{M_{pp}} p^2 + \mathrm{M_{rr}} r^2 + \mathrm{M_{uu}} u^2 + \mathrm{M_{vv}} v^2 + \mathrm{M_{qV}} q\mathrm{V} \\ & + \mathrm{M_{wV}} w\mathrm{V} + \mathrm{M_{pr}} pr + \mathrm{M_{uq}} uq + \mathrm{M_{vp}} vp + \mathrm{M_{vr}} vr \\ & + \mathrm{M_{uw}} uw + \mathrm{M_{|w|V}} |w|\mathrm{V} + \mathrm{M_{q|q|}} q|q| + \mathrm{M_{u|w|}} u|w| \\ & + \mathrm{M_{wV\overline{\eta}}} w\mathrm{V}(\overline{\eta} - 1) + \mathrm{M_{uq\overline{\eta}}} uq(\overline{\eta} - 1) \\ & + \mathrm{M_{uw\overline{\eta}}} uw(\overline{\eta} - 1)\end{aligned}$$

$$\begin{aligned}\tau^{\mathrm{N}}(v) = {} & \mathrm{N_{uu}} u^2 + \mathrm{N_{rV}} r\mathrm{V} + \mathrm{N_{vV}} v\mathrm{V} + \mathrm{N_{pq}} pq + \mathrm{N_{qr}} qr \\ & + \mathrm{N_{up}} up + \mathrm{N_{ur}} ur + \mathrm{N_{vq}} vq + \mathrm{N_{wp}} wp + \mathrm{N_{wr}} wr \\ & + \mathrm{N_{uv}} uv + \mathrm{N_{vw}} vw + \mathrm{N_{r|r|}} r|r| + \mathrm{N_{vV\overline{\eta}}} v\mathrm{V}(\overline{\eta} - 1) \\ & + \mathrm{N_{ur\overline{\eta}}} ur(\overline{\eta} - 1) + \mathrm{N_{uv\overline{\eta}}} uv(\overline{\eta} - 1)\end{aligned}$$

5) Coe: The Coe damping model, presented in [3], is based on a Taylor series expansion and assumes port/starboard vehicle symmetry.

$$\begin{aligned}\tau^{\mathrm{X}}(v) = {} & \mathrm{X_{uu}} u^2 + \mathrm{X_{vv}} v^2 + \mathrm{X_{ww}} w^2 + \mathrm{X_{pp}} p^2 + \mathrm{X_{qq}} q^2 \\ & + \mathrm{X_{rr}} r^2 + \mathrm{X_{u|u|}} u|u| + \mathrm{X_{w|w|}} w|w| + \mathrm{X_{q|q|}} q|q|\end{aligned}$$

where damping forces and moments τ^{Z} and τ^{M} are defined by replacing X with Z and M.

$$\tau^{\mathrm{Y}}(v) = \mathrm{Y_{v|v|}} v|v| + \mathrm{Y_{p|p|}} p|p| + \mathrm{Y_{r|r|}} r|r|$$

where damping moments τ^{K} and τ^{N} are defined by replacing Y with K and N.

6) Prestero: The Prestero damping model, shown in [4], includes axial drag, crossflow drag, and body lift.

$$\tau^{\mathrm{X}}(v) = \mathrm{X_{qq}} q^2 + \mathrm{X_{wq}} wq + \mathrm{X_{rr}} r^2 + \mathrm{X_{vr}} vr + \mathrm{X_{u|u|}} u|u|$$

$$\begin{aligned}\tau^{\mathrm{Y}}(v) = {} & \mathrm{Y_{v|v|}} v|v| + \mathrm{Y_{pq}} pq + \mathrm{Y_{ur}} ur + \mathrm{Y_{wp}} wp + \mathrm{Y_{uv}} uv \\ & + \mathrm{Y_{r|r|}} r|r|\end{aligned}$$

where damping moment τ^{N} is defined by replacing Y with N.

$$\begin{aligned}\tau^{\mathrm{Z}}(v) = {} & \mathrm{Z_{w|w|}} w|w| + \mathrm{Z_{pr}} pr + \mathrm{Z_{uq}} uq + \mathrm{Z_{vp}} vp + \mathrm{Z_{uw}} uw \\ & + \mathrm{Z_{q|q|}} q|q|\end{aligned}$$

where damping moment τ^{M} is defined by replacing Z with M.

$$\tau^{\mathrm{K}}(v) = \mathrm{K_{p|p|}} p|p|$$

7) Uncoupled: The uncoupled damping model assumes that motion in each axis is only dependent on velocity along that axis.

$$\begin{aligned}\tau(v) = {} & \mathrm{diag}([\mathrm{X}_u \ \mathrm{Y}_v \ \mathrm{Z}_w \ \mathrm{K}_p \ \mathrm{M}_q \ \mathrm{N}_r])v \\ & + v^{\mathsf{T}}\mathrm{diag}([\mathrm{X}_{uu} \ \mathrm{Y}_{vv} \ \mathrm{Z}_{ww} \ \mathrm{K}_{pp} \ \mathrm{M}_{qq} \ \mathrm{N}_{rr}])v \\ & + \mathrm{diag}([\mathrm{X}_{|u|} \ \mathrm{Y}_{|v|} \ \mathrm{Z}_{|w|} \ \mathrm{K}_{|p|} \ \mathrm{M}_{|q|} \ \mathrm{N}_{|r|}])|v| \\ & + v^{\mathsf{T}}\mathrm{diag}([\mathrm{X}_{u|u|} \ \mathrm{Y}_{v|v|} \ \mathrm{Z}_{w|w|} \ \mathrm{K}_{p|p|} \ \mathrm{M}_{q|q|} \ \mathrm{N}_{r|r|}])|v|\end{aligned}$$

8) Fossen: The Fossen damping model, as proposed in [5], is uncoupled. The Fossen model assumes that the vehicle is performing non-coupled motions and has three planes of symmetry.

$$\begin{aligned}\tau(v) &= \mathrm{diag}([\mathrm{X}_u\ \mathrm{Y}_v\ \mathrm{Z}_w\ \mathrm{K}_p\ \mathrm{M}_q\ \mathrm{N}_r])v \\ &\quad + |v|^\mathsf{T}\mathrm{diag}([\mathrm{X}_{u|u|}\ \mathrm{Y}_{v|v|}\ \mathrm{Z}_{w|w|}\ \mathrm{K}_{p|p|}\ \mathrm{M}_{q|q|}\ \mathrm{N}_{r|r|}])v\end{aligned}$$

We want to determine if one damping model is superior to other models for the case of streamlined AUVs, and further compare two different methods for estimating the parameters of the models. Let $\hat{v} \in \mathbb{R}^{6\times 1}$ be the estimated linear and angular velocities, and let $\overline{n}$ represent the number of damping coefficients in matrix K. As a performance metric, we utilize the root mean square (RMS) error between $\hat{v}$ and v defined in Section V-C, and the number of damping coefficients in matrix K, $\overline{n}$, to gauge model complexity.

III. Least-Squares Method

Using Assumption 1 (a), (b), (d), (e), and (f) from Section II-A, we rewrite (1) and represent the damping term $\tau(v(t))$ as

$$\tau(v(t)) = M\dot{v}(t) - \mathcal{H}(Mv(t))v(t) - \mathcal{G}(R(t)) - u(t). \quad (3)$$

We write the estimate of the damping term as $\hat{\tau}(v(t)) = \hat{K}\xi(v(t))$ and the estimation error $\tilde{\tau}(t)$ as

$$\tilde{\tau}(t) = \hat{\tau}(v(t)) - \tau(v(t)) \quad (4)$$

$$\tilde{\tau}(t) = \hat{K}\xi(v(t)) - \tau(v(t)). \quad (5)$$

Next, we express the variables that change with time in (5) as matrices. These matrices contain all the samples collected for that variable. Let

$$v_* = [v(0), v(1), ..., v(n_k)] \in \mathbb{R}^{6\times n_k} \quad (6)$$

$$\tilde{\tau}_* = [\tilde{\tau}(0), \tilde{\tau}(1), ..., \tilde{\tau}(n_k)] \in \mathbb{R}^{6\times n_k} \quad (7)$$

$$\tau_* = [\tau(0), \tau(1), ..., \tau(n_k)] \in \mathbb{R}^{6\times n_k} \quad (8)$$

$$\xi_* = [\xi(v(0)), \xi(v(1)), ..., \xi(v(n_k))] \in \mathbb{R}^{n_\xi\times n_k} \quad (9)$$

be matrix representations of the time series, where n_k is the number of samples collected and n_ξ is the number of elements in the basis vector. By substituting the matrix time series equations (6) - (9), using the vec() operator defined in [6], and using the Kronecker product also defined in [6], equation (5) can be expressed as

$$\begin{aligned}\tilde{\tau}_* &= \hat{K}\xi_* - \tau_* \\ \tilde{\tau}_*^\mathsf{T} &= \xi_*^\mathsf{T}\hat{K}^\mathsf{T} - \tau_*^\mathsf{T} \\ \mathrm{vec}(\tilde{\tau}_*^\mathsf{T}) &= \mathrm{vec}(\xi_*^\mathsf{T}\hat{K}^\mathsf{T} - \tau_*^\mathsf{T}) \\ \mathrm{vec}(\tilde{\tau}_*^\mathsf{T}) &= \mathrm{vec}(\xi_*^\mathsf{T}\hat{K}^\mathsf{T}) - \mathrm{vec}(\tau_*^\mathsf{T}) \\ \mathrm{vec}(\tilde{\tau}_*^\mathsf{T}) &= (\mathbb{I}_6 \otimes \xi_*^\mathsf{T})\mathrm{vec}(\hat{K}^\mathsf{T}) - \mathrm{vec}(\tau_*^\mathsf{T}) \quad (10)\end{aligned}$$

where $\mathbb{I}_6 \in \mathbb{R}^{6\times 6}$ is the identity matrix.

To represent different damping models, we introduce a masking matrix $M_m \in \mathbb{B}^{\overline{n}\times 6n_\xi}$, where $\mathbb{B} = \{0, 1\}$. That is, M_m is a matrix composed of only zeros and ones. Each row of M_m has exactly one non-zero element, which is equal to one. The non-zero element selects the corresponding basis function of the specific model. Equation (10) can be expressed with this masking matrix as

$$\mathrm{vec}(\tilde{\tau}_*^\mathsf{T}) = (\mathbb{I}_6 \otimes \xi_*^\mathsf{T})M_m^\mathsf{T}M_m\mathrm{vec}(\hat{K}^\mathsf{T}) - \mathrm{vec}(\tau_*^\mathsf{T}) \quad (11)$$

Using a change of variables, we setup the synthesis model

$$\begin{aligned}\tilde{\sigma} &= \mathrm{vec}(\tilde{\tau}_*^\mathsf{T}) \in \mathbb{R}^{6n_k} \\ \sigma &= \mathrm{vec}(\tau_*^\mathsf{T}) \in \mathbb{R}^{6n_k} \\ \Xi &= (\mathbb{I}_6 \otimes \xi_*^\mathsf{T})M_m^\mathsf{T} \in \mathbb{R}^{6n_k\times\overline{n}} \\ \hat{\kappa} &= M_m\mathrm{vec}(\hat{K}^\mathsf{T}) \in \mathbb{R}^{\overline{n}} \quad (12) \\ \tilde{\sigma} &= \Xi\hat{\kappa} - \sigma \quad (13)\end{aligned}$$

where $\tilde{\sigma} \in \mathbb{R}^{6n_k}$ is the vector of residual forces and moments, $\Xi \in \mathbb{R}^{6n_k\times\overline{n}}$ contains all basis functions for a particular damping model, $\hat{\kappa} \in \mathbb{R}^{\overline{n}}$ is the set of coefficients, and $\overline{n}$ is the number of coefficients for a given model, which we refer to as the model complexity. The original coefficient matrix $\hat{K}$ is recovered from $\hat{\kappa}$ using

$$\hat{K} = \mathrm{vec}^{-1}(M_m^\mathsf{T}\hat{\kappa})^\mathsf{T}, \quad (14)$$

where $\mathrm{vec}^{-1}()$ is also defined in [6].

Our goal with the least-squares method is to find the coefficient vector $\hat{\kappa}$ that minimizes residual forces and moments column vector $\tilde{\sigma}$ in (13). Recall that in order to use the offline estimator least-squares method, $\dot{v}$ must be instrumented or calculated.

IV. Adaptive Identifier Method

The adaptive identifier requires fewer instrumented variables than the least-squares approach, and thus we seek to evaluate its performance to determine if it might be useful in practice. The adaptive identifier that we use for online damping model estimation is a modest specialization of the adaptive identifier proposed in [1]. We briefly describe the identifier. For notational convenience, explicit dependence on time is omitted in this section except for the initial time.

A. Adaptive Identification System

Let $\hat{v} \in \mathbb{R}^{6\times 1}$ be the estimated linear and angular velocities. For this section, we assume the damping forces and moments $\tau(v)$ can be expressed as $K\xi(v)$ which is a linear combination of linear and angular velocity. The $\tau(v) = K\xi(v)$ assumption is not entirely true, but as shown in our experimental results, the assumption works reasonably well. Using Assumption 1 (a), (c), (d), (e), and (f) from Section II-A and Assumption 2 (a) and (b) from Section II-B, consider the following adaptive identifier for the damping coefficients based on equation (1)

$$M\dot{\hat{v}} = \mathcal{H}(Mv)v + \hat{K}\xi(v) + \mathcal{G}(R) + u - a\Delta v \quad (15)$$

$$\dot{\hat{K}} = -\gamma\Delta v\xi(v)^\mathsf{T} \quad (16)$$

where $\hat{K}\xi(v)$ is the estimate of the damping term $\tau(v)$, $\Delta v = \hat{v} - v$, $\Delta K = \hat{K} - K$, a and $\gamma \in \mathbb{R}_+$, and $\hat{v}(t_0) = v(t_0)$. We define an error system by subtracting equation (1) from (15)

$$\begin{aligned}M\dot{\hat{v}} - M\dot{v} &= \mathcal{H}(Mv)v + \hat{K}\xi(v) + \mathcal{G}(R) + u - a\Delta v\\ &\quad - \mathcal{H}(Mv)v - K\xi(v) - \mathcal{G}(R) - u\\ M(\dot{\hat{v}} - \dot{v}) &= (\hat{K} - K)\xi(v) - a\Delta v\\ M\dot{\Delta}v &= \Delta K\xi(v) - a\Delta v.\end{aligned} \tag{17}$$

Recall that K is assumed to be constant. This assumption implies that $\dot{\Delta}K = \dot{\hat{K}}$. Also, recall that M^{-1} exists because M is a positive-definite matrix. Solving for $\dot{\Delta}v$ by multiplying both sides of equation (17) by M^{-1} and using (16) yields the error system

$$\dot{\Delta}v = M^{-1}(\Delta K\xi(v) - a\Delta v) \tag{18}$$

$$\dot{\Delta}K = -\gamma\Delta v\xi(v)^{\mathsf{T}}. \tag{19}$$

We show that the error system (18) and (19) is uniformly stable at the equilibrium point $\Delta v = 0_{6\times 1}$, $\Delta K = 0_{6\times n_\xi}$ by Lyapunov's Direct Method. Using Barbalat's Lemma, we show that $\lim_{t\to\infty}\Delta v = 0_{6\times 1}$. Finally, we show that $\lim_{t\to\infty}\dot{\Delta}K = 0_{6\times n_\xi}$ which means the damping coefficients converge to constant values. However, this does not guarantee convergence to the real damping coefficients.

B. Convergence of the Error System

The proof presented here is a specialization of the more general results that appear in [1].

Proposition 1. *Consider the equilibrium point* $\Delta v = 0_{6\times 1}$, $\Delta K = 0_{6\times n_\xi}$ *for the nonlinear nonautonomous system*

$$\begin{aligned}\dot{\Delta}v &= M^{-1}(\Delta K\xi(v) - a\Delta v)\\ \dot{\Delta}K &= -\gamma\Delta v\xi(v)^{\mathsf{T}}.\end{aligned} \tag{20}$$

If $a, \gamma \in \mathbb{R}_+$*, and using Assumption 1 (a), (c), (d), (e), and (f) from Section II-A and Assumption 2 (a) and (b) from Section II-B, then the*

1) *system* (20) *is uniformly stable at* $\Delta v = 0_{6\times 1}$, $\Delta K = 0_{6\times n_\xi}$
2) $\lim_{t\to\infty}\Delta v = 0_{6\times 1}$
3) $\lim_{t\to\infty}\dot{\Delta}K = 0_{6\times n_\xi}$.

Proof. Choose the following candidate Lyapunov function for the error system (20)

$$V = \frac{1}{2}\Delta v^{\mathsf{T}} M\Delta v + \frac{1}{2\gamma}\operatorname{tr}(\Delta K\Delta K^{\mathsf{T}}). \tag{21}$$

Equation (21) is positive-definite, decrescent, smooth, and thus V is equal to zero if and only if $\Delta v = 0_{6\times 1}$ and $\Delta K = 0_{6\times n_\xi}$. Calculating the time derivative along trajectories from equation (21) yields

$$\dot{V} = \Delta v^{\mathsf{T}} M\dot{\Delta}v + \frac{1}{\gamma}\operatorname{tr}(\Delta K\dot{\Delta}K^{\mathsf{T}}). \tag{22}$$

By substituting (20) into (22), and recalling the property $\operatorname{tr}(AB) = \operatorname{tr}(BA)$ for conformable matrices, we write

$$\begin{aligned}\dot{V} &= \Delta v^{\mathsf{T}} M\dot{\Delta}v + \frac{1}{\gamma}\operatorname{tr}(\Delta K\dot{\Delta}K^{\mathsf{T}})\\ &= \Delta v^{\mathsf{T}} M\left[M^{-1}(\Delta K\xi(v) - a\Delta v)\right] + \frac{1}{\gamma}\operatorname{tr}(\Delta K\dot{\Delta}K^{\mathsf{T}})\\ &= \Delta v^{\mathsf{T}}\Delta K\xi(v) - a\Delta v^{\mathsf{T}}\Delta v + \frac{1}{\gamma}\operatorname{tr}(\Delta K\left[-\gamma\Delta v\xi(v)^{\mathsf{T}}\right]^{\mathsf{T}})\\ &= \Delta v^{\mathsf{T}}\Delta K\xi(v) - a\Delta v^{\mathsf{T}}\Delta v - \operatorname{tr}(\Delta K\xi(v)\Delta v^{\mathsf{T}})\\ &= \Delta v^{\mathsf{T}}\Delta K\xi(v) - a\Delta v^{\mathsf{T}}\Delta v - \operatorname{tr}(\Delta v^{\mathsf{T}}\Delta K\xi(v))\\ &= \Delta v^{\mathsf{T}}\Delta K\xi(v) - a\Delta v^{\mathsf{T}}\Delta v - \Delta v^{\mathsf{T}}\Delta K\xi(v)\\ &= -a\Delta v^{\mathsf{T}}\Delta v.\end{aligned} \tag{23}$$

$\dot{V}$ is negative semi-definite because it is not a function of all the state variables. By Lyapunov's Direct Method [7], we conclude that the error system (20) is uniformly stable at the equilibrium point $\Delta v = 0_{6\times 1}$, $\Delta K = 0_{6\times n_\xi}$.

To show that $\lim_{t\to\infty}\Delta v = 0_{6\times 1}$, we use Barbalat's Lemma. We need to show that Δv, $\dot{\Delta}v \in \mathcal{L}^\infty$ and $\Delta v \in \mathcal{L}^p$. Equations (21) and (23) show that Δv and ΔK are bounded by Lyapunov's Direct Method. Therefore, $\Delta v \in \mathcal{L}^\infty$. Equations (21) and (23) also imply that V is bounded below and non-increasing. Using Lemma 3.2.3 from [7], we conclude that the $\lim_{t\to\infty} V$ exists. Integrating equation (23) from zero to t and taking the limit of t to infinity shows that $\Delta v \in \mathcal{L}^2$. Finally, we know that v, Δv, and ΔK are bounded, and K is constant. This implies that $\hat{v}$ and $\hat{K}$ are bounded. With $\xi(v)$ bounded, we conclude from the first equation in (20) that $\dot{\Delta}v \in \mathcal{L}^\infty$. Thus, $\lim_{t\to\infty}\Delta v = 0_{6\times 1}$ by Barbalat's Lemma.

From equation (23) and the fact that Δv converges to 0, we infer that $\lim_{t\to\infty}\dot{V} = 0$. Since $\dot{V}$ converges to 0, ΔK converges to a constant and $\lim_{t\to\infty}\dot{\Delta}K = 0_{6\times n_\xi}$. This guarantees convergence of the damping coefficients to constant values but not to the real damping coefficients. □

V. Experimental Results

A. Experimental Environment

The Virginia Tech 690 AUV shown in Figure 1 and described in [8] was used to acquire the experimental data. The AUV diameter is 6.9 inches, length is 2.0 meters, and dry weight is 41.5 kilograms. It is ballasted to be slightly positively buoyant. The Virginia Tech 690 AUV has a single propeller at the stern of the vehicle, and it has four control surfaces at the tail. The mass matrix M for the vehicle comes from Appendix B in [9]. The model for the forces and moments due to the control surfaces and propeller u is found in Section 2.3 and Appendix B in [9]. The AUV employs an H_∞ autopilot that minimizes pitch and yaw coupling [10].

The 690 AUV is equipped with a Doppler velocity log (DVL), that measures bottom relative velocity. The vehicle also has an attitude and heading reference sensor (AHRS) that measures attitude, body relative rotation rates, and translation accelerations. The 690 does not have a sensor that measures angular acceleration. Angular acceleration is estimated by finite differences of angular velocity measurements.

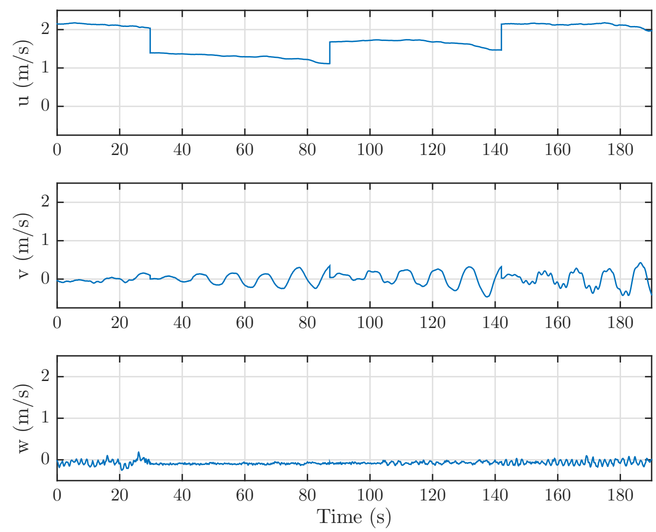

Fig. 2. Translation velocity damping parameter estimation data set

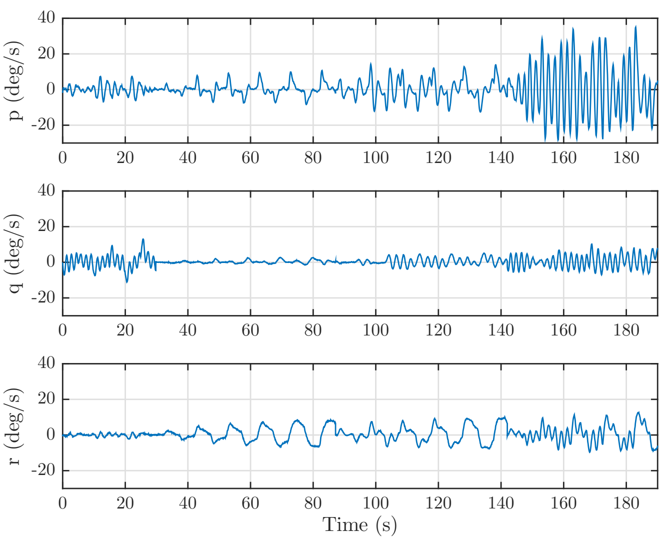

Fig. 3. Rotational velocity damping parameter estimation data set

B. Data Sets

Data was acquired during experiments performed at Claytor Lake in Pulaski County, Virginia. The data collected from the experiments was partitioned into a set that is used for estimating damping parameters and another set that is used to validate estimated damping parameters. The data set used for damping parameter estimation is shown in Figures 2 and 3. The estimation data set is a concatenation of four independent data sets. The first data set is composed of depth steps at a propeller speed of 2600 rpm, and the three remaining sets are composed of yaw steps at propeller speeds of 1800, 2133, and 2600 rpm respectively. The concatenation produces discontinuities three times in the data.

With the damping parameter estimation data set, we apply the least-squares synthesis model (12) and (13) to find the value of $\hat{\kappa}$ that minimizes the residual force for each damping model that is described in Section II-C. From the minimizing $\hat{\kappa}$, we construct the coefficient matrix $\hat{K}$ for each model using the inverse equation (14).

The adaptive identification algorithm is initialized with the initial velocity measurements. The first six columns of $\hat{K}$ are initialized to $-\mathbb{I}_6$. The remaining elements of $\hat{K}$ are initialized to zero. Adaption gains are $a = 20$ and $\gamma = 20$.

The data reserved for validation has two sections. The first section consists of a series of step changes in depth with constant propellor speed 2133 rpm. The second section contains yaw steps at a propeller speed of 2350 rpm. The linear damping model results are shown in Figures 4 and 5. For the other damping models, we show only numerical performance metrics that are described in Section V-C.

C. Experimental Results

The performance metrics to compare models were model complexity $\overline{n}$, and the root mean square (RMS) error of the linear and the angular velocities. The RMS error is defined

$$J(\Delta v) = \sqrt{\frac{1}{6n_k} \sum_{i=1}^{6n_k} (\mathrm{vec}(\Delta v))_i^2} \tag{24}$$

where n_k is the number of time samples and $\mathrm{vec}(\Delta v) \in \mathbb{R}^{6n_k}$ stacks the vectors into one column.

Table I shows the RMS error for the different damping models. The table is ordered by the number of coefficients for the specific model $\overline{n}$. With the use of a limited data set and only one vehicle, our results are only first impressions. The results in Table I suggest that the performance of both identification methods is similar.

From the table and our two metrics, we can immediately draw conclusions of the relative performance between models. The Coe, Prestero, uncoupled, and Fossen models have the fewest number of damping parameter coefficients and perform worse than the other models. The uncoupled and Fossen models assume motion in each axis is independent. Clearly, there is coupling between axes which explains the poor performance of these models in addition to the limited number of coefficients. The Coe model assumes port and starboard vehicle symmetry, which is the case for the 690 AUV, to simplify the equations of motion. With these simplifications, the Coe model performs similarly to the Prestero model.

The pitch-yaw model has a large number of coefficients, but does not exhibit the same performance as the McFarland-Whitcomb or Gertler-Hagen model. The pitch-yaw model superimposes separate models for pitch and yaw. The model assumes no x-axis damping moment will occur and leads to no coefficients for the $\tau^{\mathrm{K}}(v)$ moment in the $\hat{K}$ matrix. Therefore, the pitch-yaw model cannot account for any residual x-axis moment. An improved model would include some coefficients in this degree of freedom to increase tracking performance.

The McFarland-Whitcomb, Gertler-Hagen, and linear models have similar error values. The McFarland-Whitcomb and Gertler-Hagen models achieve the lowest RMS error; however, both contain more coefficients than the linear damping model.

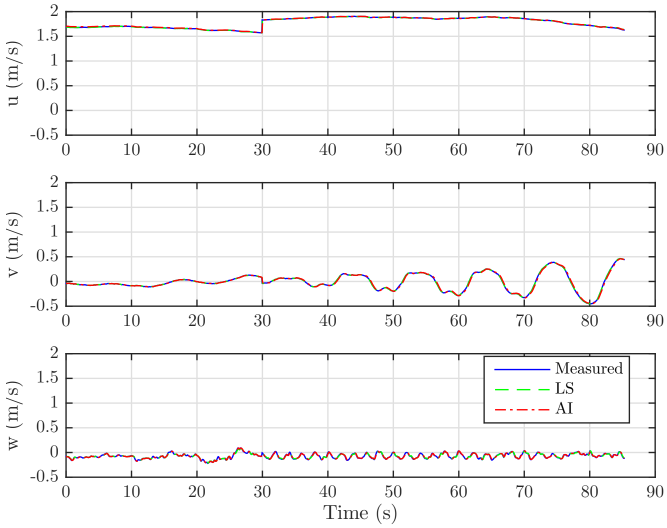

Fig. 4. Translation velocity validation plots for the linear damping model. The solid line is the measurement. The dashed line is the least-squares estimate. The dashed-dot line is the adaptive identifier estimate.

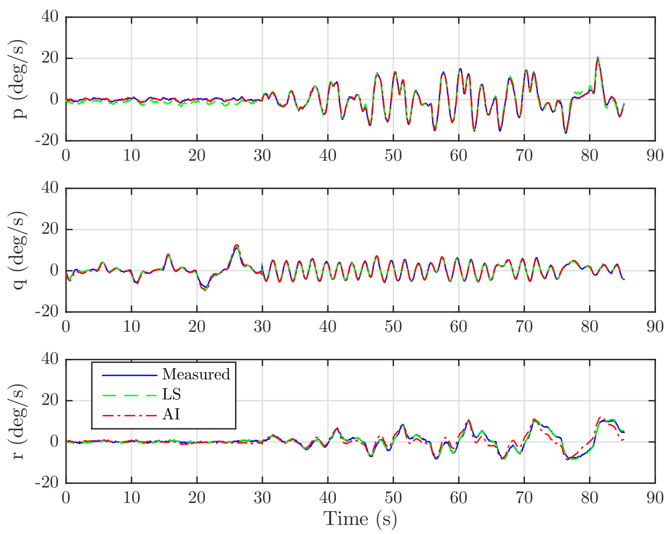

Fig. 5. Rotational velocity validation plots for the linear damping model. The solid line is the measurement. The dashed line is the least-squares estimate. The dashed-dot line is the adaptive identifier estimate.

The Gertler-Hagen model calculates coupled velocities to estimate the forces and moments, and it has similar performance to the McFarland-Whitcomb model with less coefficients. One remarkable conclusion we can draw from the results is the linear damping model performs similarly to the McFarland-Whitcomb and Gertler-Hagen models but with significantly less coefficients.

VI. Conclusion

This paper presents a comparison of different hydrodynamic damping models by applying a least-squares method and an adaptive identification method. Our results should be considered preliminary due to the use of a limited data set and only one vehicle. From the results, the linear damping model performance is similar to the McFarland-Whitcomb and Gertler-Hagen but employs fewer coefficients. The linear damping model is preferred over other models due to its simplicity.

The least-squares and adaptive identification methods are also compared. The least-squares method is an off-line method that requires the instrumentation or calculation of angular acceleration. Adaptive identification can be implemented for online estimation and generates similar results to the least-squares method. The adaptive identifier might be preferred for some applications because it does not require angular acceleration.

TABLE I
Root Mean Square velocity error values for different models

Damping Model	$\overline{n}$	LS error	AI error
McFarland-Whitcomb	216	0.40	0.54
Pitch-Yaw	100	1.74	2.00
Gertler-Hagen	88	0.39	0.55
Linear	36	0.50	0.74
Coe	33	1.29	2.29
Prestero	30	1.79	2.31
Uncoupled	24	2.15	1.98
Fossen	12	2.24	2.08

References

[1] C. McFarland and L. Whitcomb, “Comparative experimental evaluation of a new adaptive identifier for underwater vehicles,” in *Robotics and Automation (ICRA), 2013 IEEE International Conference on*, May 2013, pp. 4614–4620.

[2] M. Gertler and G. R. Hagen, “Standard equations of motion for submarine simulation,” DTIC Document, Tech. Rep., 1967.

[3] R. G. Coe, “Improved underwater vehicle control and maneuvering analysis with computational fluid dynamics simulations,” Ph.D. dissertation, Virginia Polytechnic Institute and State University.

[4] T. Prestero, “Development of a six-degree of freedom simulation model for the remus autonomous underwater vehicle,” in *OCEANS, 2001. MTS/IEEE Conference and Exhibition*, vol. 1. IEEE, 2001, pp. 450–455.

[5] T. I. Fossen, *Guidance and control of ocean vehicles*. Chichester; New York: Wiley, 1994.

[6] A. Graham, *Kronecker products and matrix calculus: with applications*. Horwood England, UK, 1981, vol. 108.

[7] A. I. Petros and J. Sun, *Robust adaptive control*. PTR Prentice-Hall, 1996.

[8] B. McCarter, S. Portner, W. L. Neu, D. J. Stilwell, D. Malley, and J. Mims, “Design elements of a small auv for bathymetric surveys,” in *Autonomous Underwater Vehicles (AUV), 2014 IEEE/OES*. IEEE, 2014, pp. 1–5.

[9] B. R. McCarter, “Experimental evaluation of viscous hydrodynamic force models for autonomous underwater vehicles,” Master’s thesis, Virginia Polytechnic Institute and State University.

[10] J. Petrich and D. J. Stilwell, “Robust control for an autonomous underwater vehicle that suppresses pitch and yaw coupling,” *Ocean Engineering*, vol. 38, no. 1, pp. 197–204, 2011.